Contributions to the theory of aircraft structures

Buckling of circular cylindrical shells under axial compression*

Bernard Budiansky and John W. Hutchinson

ABSTRACT

Buckling and postbuckling behavior under axial compression is analyzed for a long circular cylinder containing an axisymmetric imperfection. Bifurcation stresses are investigated for all possible modes, both periodic and aperiodic, and postbuckling analysis reveals that bifurcation is not always associated with a loss of load-carrying capacity. The results provide some theoretical foundation for empirical knockdown factors.

INTRODUCTION

The notion of a 'knockdown factor' was introduced long ago in the field of shell buckling to come to grips in a practical way with the highly unpredictable behavior of shell structures. This notion is still in use and as recently as 1968 the U.S. National Aeronautics and Space Administration released a special report on design criteria based on this concept[1]. The knockdown factor is chosen so that the product of it and the classical buckling load leads to a lower bound to all the existing experimental data for that configuration. An enormous amount of data for this purpose has been collected for the monocoque cylindrical shell under axial compression (see, for example, Weingarten, Morgan and Seide[2]) and knockdown factors of 1/4 or 1/3 are typical for all but extremely thin shells.

Is there any real physical basis to such factors; or are they simply empirical lower bounds which will become even lower as more data is accumulated? Considerable effort has been expended in attempts to answer this question, and the current view of the buckling of axially compressed cylinders seems to favor the second interpretation.

Two kinds of theoretical results bolster this conclusion. The idea that the minimum postbuckling load of the perfect cylindrical shell is closely related to the maximum support load of a highly imperfect cylinder was popular for a number of years. However, as more and more accurate calculations were carried out, the predicted minimum of the postbuckling load turned out to be well below the accepted empirical knockdown loads. The last calculation of this type, by Hoff, Madsen and Mayers[3], suggests that the minimum postbuckling load may even vanish as the thickness to radius ratio approaches zero.

More recently the emphasis in shell buckling has been on the analysis of the nonlinear buckling behavior of imperfect shells. However, very few accurate results, either analytical or numerical, are available for assessing behavior in the range where the imperfection level is such that the buckling load is reduced below, say, 25 percent of the classical. One notable exception is Koiter's[4] work on cylindrical shells with axisymmetric sinusoidal imperfections. Koiter obtained a relatively simple formula for an upper bound to the load at which nonaxisymmetric bifurcation from the axisymmetric state occurs. Imperfection amplitudes of just one shell thickness reduce the bifurcation load to a fifth of the classical load. Further, Koiter found that as the imperfections get still larger, the bifurcation stress approaches one tenth of the classical value. Thus, while a cylindrical shell with an axisymmetric sinusoidal imperfection is admittedly an idealized model, there is, nevertheless, nothing about Koiter's upper bound which attaches any theoretical significance to any knockdown factor except possibly the limit value of 1/10 for large imperfections.

The above discussion, however, embodies the tacit assumption that the collapse load of the imperfect shell coincides with the bifurcation load. This need not be the case. Certainly if the imperfection is sufficiently small bifurcation is unstable and is equivalent to collapse, but the central conclusion of the present paper is that for sufficiently large imperfections the bifurcation from the axisymmetric state is initially stable, so that loads above the bifurcation load can be sustained. The combined picture involving bifurcation and postbuckling results to be presented suggests a qualitative theoretical rationale for the empirical knockdown factors.

We follow Koiter[4] and consider the infinitely long cylindrical shell under axial compression with axisymmetric sinusoidal imperfections. The bifurcation problem is formulated exactly and a complete family of buckling modes is identified. Koiter's upper bound pertains to the critical stress associated with one restricted set of modes, and the critical stress for a set of long wavelength modes reproduces some numerical results obtained by Almroth [5]. The initial postbuckling analysis is also formulated exactly. An exact analytical solution is obtained for the limiting case of modes with infinitely long wavelengths, and numerical analysis is used to solve the equations for the other cases. The body of the paper includes only a summary of the results and their interpretation. Details of the analysis are given in the Appendix.

BUCKLING AND POSTBUCKLING BEHAVIOR: RESULTS AND DISCUSSION

Bifurcation behavior

The classical analysis of the buckling of an infinitely long cylindrical shell of radius R and thickness t subject to a compressive stress σ yields the critical bifurcation stress

$$\sigma_{c1} = \frac{E}{\sqrt{3(1-v^2)}} \frac{t}{R} \tag{1}$$

where E is Young's modulus and v is Poisson's ratio. A multiplicity of buckling modes is associated with σ_{c1}. The normal component of deflection W for these modes has the form

$$W = tw_1 = t \cos\left(\frac{kx}{2}\right) \cos\left(\frac{s_0 y}{2}\right) \tag{2}$$

where x and y are dimensionless axial and circumferential coordinates, respectively, defined in terms of longitudinal and circumferential distances X and Y by $x = Xq_0/R$ and $y = Yq_0/R$ where

$$q_0^2 = \sqrt{12(1-v^2)}\frac{R}{t} \tag{3}$$

The wave numbers in (2) must satisfy

$$(k-1)^2 + s_0^2 = 1 \tag{4}$$

where, for circumferential periodicity, $(q_0 s_0/2)$ must be an integer. For future reference we note that the axisymmetric mode is given by $k = 2$ and $s_0 = 0$, and the mode with a square wave pattern corresponds to $k = 1$ and $s_0 = 1$. For any other value of s_0 in the range $0 < s_0 < 1$, equation (4) has two positive roots, k_1 and k_2, that satisfy $k_1 + k_2 = 2$.

Equations (1)–(4) as well as our subsequent analysis are based on the Kármán-Donnell shell equations and consequently, as is well known, these results are restricted to modes with more than, say, four wavelengths around the circumference.

An axisymmetric imperfection in the shape of the classical axisymmetric mode is considered, i.e.,

$$\bar{W} = -\delta \cos x \tag{5}$$

The eigenvalue problem governing nonaxisymmetric bifurcation from the axisymmetric prebuckling state is formulated in the Appendix, as are the equations for the initial postbuckling behavior. For a given magnitude δ of

the axisymmetric imperfection, a mode can be written as

$$w_1 = \text{Real}\left[e^{ikx/2}w_{11}(x)\right]\cos\frac{s_0 y}{2} \tag{6}$$

where w_{11} is a complex function which is periodic in x with period 2π. Values of k in the range $0 \leq k \leq 1$ generate all possible bifurcation modes, both periodic and aperiodic in x. Note that the classical modes (2) of the perfect cylinder can be recovered from (6) by setting $w_{11} = 1$. Note further that letting $w_{11} = A + Be^{-ix}$ in (6) with $s = s_0$ yields the form

$$w_1 = \left\{A\cos\left[\frac{kx}{2}\right] + B\cos\left[\frac{(2-k)x}{2}\right]\right\}\cos\frac{s_0 y}{2} \tag{7}$$

Thus, (6) can also represent any linear combination of the two modes of the perfect cylinder associated with a given value of s_0. In general, the axial variation of such a mode is not periodic.
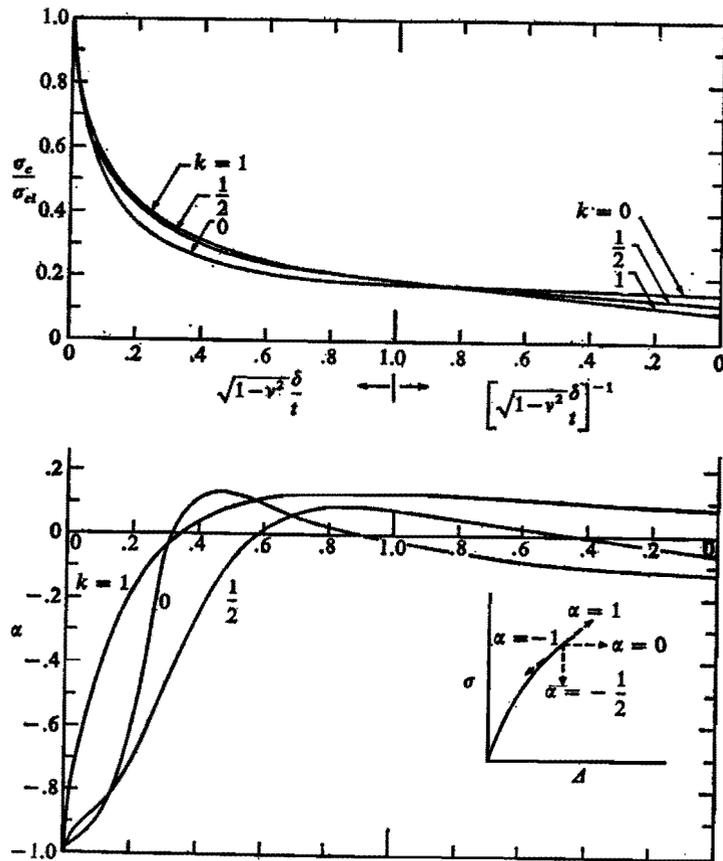

Figure 1. Buckling and postbuckling of imperfect cylindrical shells under axial compression

Calculations for the imperfect cylinder are described in the Appendix. Curves giving the bifurcation stress σ_c (normalized by the classical buckling stress σ_{c1}) associated with values of k of 0, $\frac{1}{2}$ and 1 are plotted in the top half of figure 1 as a function of $\sqrt{1-v^2}\delta/t$. In each case, for a given value of k and $\sqrt{1-v^2}\delta/t$, the value of σ_c shown represents the minimum eigenvalue found by treating the circumferential wavelength parameter s as a continuous variable. The curves marked $k = 1$ and $k = 1/2$ are the result of numerical calculations, whereas the curve for $k = 0$ in figure 1 is an exact limiting result. With $\lambda_0 = \sigma_c/\sigma_{c1}$ and $\gamma = \sqrt{12(1-v^2)}\delta/t$, the formula for this curve is

$$\gamma^4(1-6\lambda_0-4\lambda_0^2)+4\gamma^2(1-\lambda_0)^2(2-6\lambda_0-5\lambda_0^2)+16(1-\lambda_0)^7(1+\lambda_0) = 0 \tag{8}$$

Strictly speaking, this limit for $k \to 0$ has no physical meaning since it implies infinitely long wavelengths in both the axial and circumferential direction. Its usefulness, however, lies in the fact that it does provide a very good approximation for modes associated with small values of k and s which are in the range of physical validity. Furthermore, for values of $\sqrt{1-v^2}\delta/t$ less than about unity this limit provides the *lowest* eigenvalue σ_c among all possible k. This is illustrated in the upper half of figure 2 where some selected calculated results are plotted to display the variation in σ_c as a function of k for fixed values of δ/t.

For values of $\sqrt{1-v^2}\delta/t$ greater than about unity the case for $k = 1$ yields the lowest bifurcation stress σ_c. Thus over essentially the entire range of $\sqrt{1-v^2}\delta/t$ the critical (lowest) bifurcation stress is given either by the case for $k = 0$ or for $k = 1$. The companion curve for $k = \frac{1}{2}$ has also been included in figure 1 even though it is only slightly displaced from that for $k = 1$. Postbuckling considerations divulge a special role for this case.

Koiter's[4] upper bound calculation took into account modes in the $k = 1$ class and his results are exceedingly close to those shown in figure 1 for this case. In fact, the absolute discrepancy is never greater than that associated with the limit for $\delta \to \infty$, where Koiter's upper bound predicts $\sigma_c/\sigma_{c1} = 1/10$ and the numerical result is $\sigma_c/\sigma_{c1} = 0.0958$.

Almroth[5] extended Koiter's analysis to include certain long wavelength modes and he found buckling modes which fit the description given by (6) with low k values. For values of $\sqrt{1-v^2}\,\delta/t$ less than about 0.8 Almroth's results fall on the curve labeled $k = 0$ in the upper half of figure 1.*

As mentioned above, the circumferential wavelength parameter s is treated as a continuous variable in all our numerical calculations in the search for the minimum eigenvalue. For completeness we include in figure 3

---

* For values of δ/t between about .8 and 1 Almroth shows values of σ_c/σ_{c1} lower than those shown by the curve for $k = 0$; however, we have not discovered any bifurcation stresses in this range lower than those found for $k = 0$.

curves of the minimizing value of s as a function of the imperfection amplitude. If, as shown on the ordinate, s is normalized by s_0, the value associated with the perfect cylinder (4), then all curves lie between those shown for $k = 0$ and $k = 1$. In the limiting case $k \to 0$ both s and s_0 approach zero; however, the limit of the ratio s/s_0 is well defined.

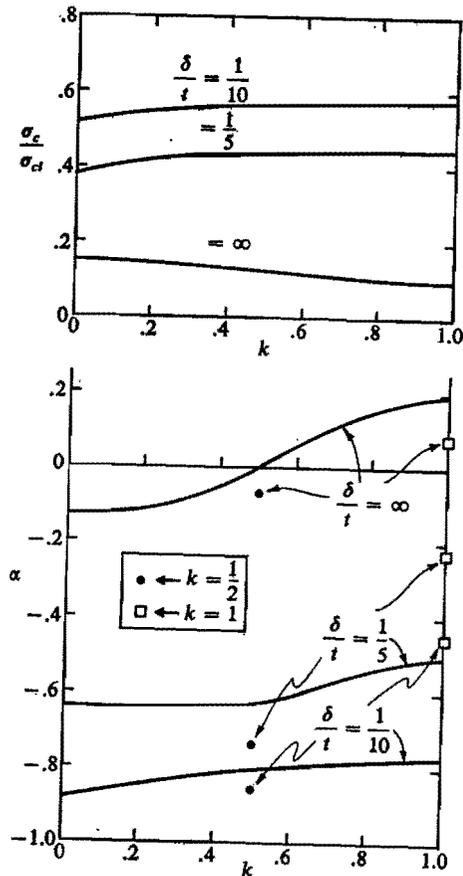*Figure 2. Variation of bifurcation stress and postbuckling parameter as a function of k for fixed values of imperfection $(v = \frac{1}{3})$*

Postbuckling behavior

As a measure of the postbuckling behavior we consider the change in overall stiffness following bifurcation. The average compressive axial stress is denoted by σ and the average axial shortening per unit length is denoted by Δ. At bifurcation the nondimensional prebuckling stiffness S_0 is given in terms

of the axisymmetric prebuckling quantities by

$$S_0 = \frac{1}{E}\left(\frac{d\sigma_0}{d\Delta_0}\right)_{\sigma=\sigma_c} \tag{9}$$

where the zero subscript refers to the prebuckling configuration. The initial postbuckling stiffness is denoted in terms of the corresponding postbuckling variables by

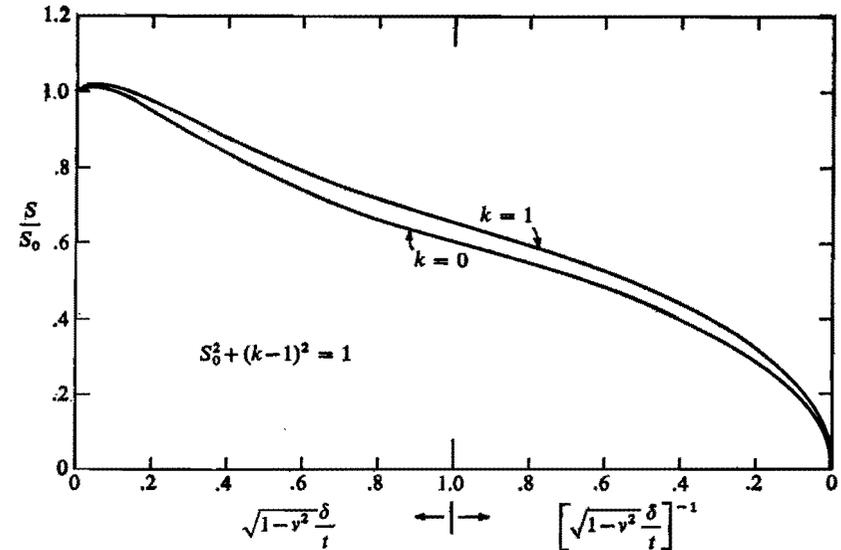$$S = \frac{1}{E}\left(\frac{d\sigma}{d\Delta}\right)_{\sigma=\sigma_c} \tag{10}$$

Figure 3. Critical circumferential wavelength parameter as a function of imperfection amplitude

A convenient measure of the relative magnitudes of the postbuckling stiffness and the prebuckling stiffness is the nondimensional parameter α where

$$\alpha = \frac{2}{\pi}\arctan\left(\frac{S}{S_0-S}\right) \tag{11}$$

As depicted in the insert in the bottom half of figure 1, α ranges from $+1$, corresponding to unchanged overall stiffness, to the most highly unstable situation at $\alpha = -1$.

Curves of α as a function of $\sqrt{1-v^2}\delta/t$ are presented in the lower half of figure 1. The curve for $k = 0$ is the plot of the exact solution for this limiting case and the other cases, for $k = \frac{1}{2}$ and 1, were obtained by numerical analysis. Both the analytical and numerical analyses are given in the Appendix.

Of the three cases shown, that for $k = 1$ is most readily interpreted. For $\sqrt{1-v^2}\,\delta/t$ less than about 0.35 (and σ_c/σ_{c1} greater than about 0.33), bifurcation into the $k = 1$ mode is unstable under dead load since the average stress falls as buckling proceeds, i.e., $\alpha < 0$. However, for values of σ_c/σ_{c1} less than about 0.33, bifurcation is stable ($\alpha > 0$) and an average stress above σ_c can be supported. Furthermore, for $\sqrt{1-v^2}\,\delta/t$ greater than about unity the lowest value of σ_c is associated with $k = 1$ and thus in this range the initial postbuckling behavior is stable.

For $\sqrt{1-v^2}\,\delta/t$ less than about unity both the limit for $k = 0$ and the case for $k = \frac{1}{2}$ yield values of σ_c which are lower than for $k = 1$. In addition, as measured by α, they generally have a more unstable postbuckling behavior. As the imperfection amplitude becomes larger both of these cases first enter a range of stable bifurcation under dead load ($\alpha > 0$) and then, for sufficiently large imperfection levels, become unstable ($\alpha < 0$) again. But at the same time, the values of σ_c associated with these two cases become larger than those for $k = 1$ and are therefore no longer critical.

Additional calculations were made to obtain the crossplots of α vs. k in figure 2, which reveal that the most unstable postbuckling behavior is associated with either the $k = 0$ limit or the case for $k = \frac{1}{2}$, depending on the value of $\sqrt{1-v^2}\,\delta/t$. The parameter α is a smooth function of k except at the isolated points $k = \frac{1}{2}$ and 1, where α has discontinuous values. (This singular behavior is discussed in the Appendix.) It appears evident from figures 1 and 2 that an assessment of the cylinder behavior can rest on study of just the results for $k = 0$, $\frac{1}{2}$ and 1.

Implications of the analysis

In figure 4 the measure of postbuckling stability α is plotted directly as a function of σ_c/σ_{c1} for each of the three important cases. By eliminating the explicit role of the imperfection in this figure we can hope that the interpretation is somewhat freed from the specific imperfection shape assumed. Figure 4 reveals a strikingly sharp transition from the *highly* unstable behavior which occurs when σ_c/σ_{c1} is greater than roughly 0.3 to the mildly unstable, or even stable, behavior for lower bifurcation stresses. The transition is most abrupt for the cases of $k = \frac{1}{2}$ and the limiting case $k = 0$ and both of these cases are far more critical in this range than for $k = 1$. Thus the values of σ_c/σ_{c1} of about 1/4 to 1/3 (corresponding to the knockdown factors often suggested) do have a special significance. Lower collapse loads are clearly possible, however. The solid dots which terminate the curves in figure 4 correspond to the limit values for $\delta \to \infty$. It is interesting to note that the lowest possible bifurcation stress for which the initial postbuckling behavior is unstable under dead load occurs for $k = \frac{1}{2}$ with $\sigma_c/\sigma_{c1} = 0.125$; this, however, is a limiting result for $\delta \to \infty$ (see fig. 2).
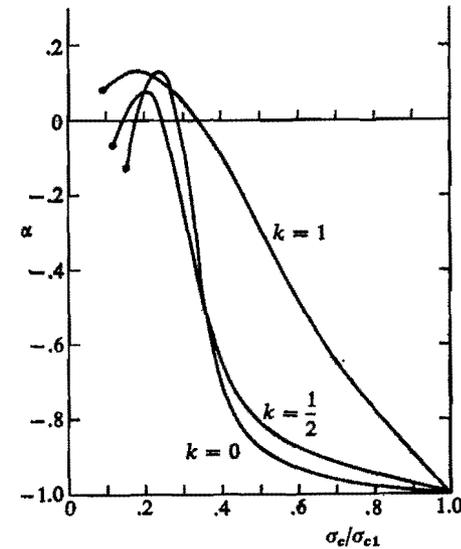

Figure 4. Postbuckling behavior as a function of buckling stress

Another feature which shows up in figure 4 is that stable initial postbuckling behavior under *prescribed axial shortening* (i.e., $\alpha > -\frac{1}{2}$) will always occur for values of σ_c/σ_{c1} less than 1/3. This result has implications for the effect of the formation of a local buckle on a cylindrical shell. Suppose such a buckle develops (due to a localized imperfection pattern) at an overall stress level below $\sigma/\sigma_{c1} = 1/3$. If it can be assumed that the local buckling region 'sees' a surrounding constraint which is approximated by the prescribed shortening condition, then local snapping will not immediately occur and, therefore, total collapse will not be precipitated.

No explicit dependence on the ratio of radius to thickness, R/t, appears in our analyses. Modes associated with low k and s values have long axial and circumferential wavelengths but these modes are physically meaningful for all but relatively thick or short shells. More to the point though is the fact that the mode associated with $k = 1/2$ *is* a short wavelength mode and this case does stand out as being the most unstable over nearly the entire range of imperfection levels. Thus it would appear unlikely that any deterministic analysis of imperfect cylinders (excluding thick or very short shells) could bring in an effect of R/t such as is observed in the experimental trends[2].

Our final conclusions drawn from this analysis with regard to knockdown factors are mixed. On the one hand, figure 4 does display a remarkable transition in behavior in the range corresponding to the most frequently used knockdown factors. On the other hand, one may still have to appeal to the presumption of increased likelihood of large imperfections for thinner

shells in order to explain observed reductions in knockdown factors with increasing values of R/t.

APPENDIX

Symbols

E	Young's modulus
v	Poisson's ratio
R	cylinder radius
t	cylinder wall thickness
X	longitudinal coordinate
Y	circumferential coordinate
q_0	$= [12(1-v^2)]^{1/4}[R/t]^{1/2}$
c	$= [3(1-v^2)]^{1/2}$
U	axial displacement
V	circumferential displacement
W	outward radial displacement
$\tilde{W}$	initial radial displacement (imperfection)
δ	amplitude of initial imperfection
F	Airy function for stress-resultants
x	$= Xq_0/R$
y	$= Yq_0/R$
w	$= W/t$
$\tilde{w}$	$= \tilde{W}/t$
f	$= [q_0^2/Et^2R]F$
γ	$= 2c\delta/t$
σ	average axial compression
σ_c	value of σ at bifurcation buckling
σ_{c1}	classical buckling stress $(= Et/cR)$
λ	$= \sigma/\sigma_{c1}$
λ_c	$= \sigma_c/\sigma_{c1}$
ξ	amplitude of buckling displacement
b	postbuckling coefficient (eq. (A4))
α	postbuckling stiffness indicator (eq. (11))
k	longitudinal wave number (eq. (A7))
s	circumferential wave number (eq. (A7))
ρ	$= \gamma s^2$
τ	$= 2k/s^2$
Δ	average shortening per unit length
S	postbuckling axial stiffness
S_0	prebuckling axial stiffness
N	number of intervals in finite difference scheme
h	$= \pi/N$
A_p	$= h^{-2}+\frac{1}{2}ipkh^{-1}$

Square matrices:

$$B_{pqn}, P_n, Q_n, H_n, M_{pq}$$

Column matrices:

$$Z_n, \zeta_{p,n}, T_{p,n}$$

Operators:

$$( )' = \frac{\partial( )}{\partial x}$$

$$(\dot{}) = \frac{\partial( )}{\partial y}$$

$L_p( )$ equation (A9)
$\mathcal{L}_p( )$ equation (A38)
$\langle \rangle$ denote average on the cylinder

Theoretical analysis

The nondimensionalized Kármán-Donnell equations for the cylinder containing an initial axisymmetric imperfection are

$$\begin{cases} \nabla^4 w + f'' = 2c\psi(f, w+\tilde{w}) \\ \nabla^4 f - w'' = -c\psi(w, w+2\tilde{w}) \end{cases} \quad (A1)$$

where

$$\psi(g_1, g_2) = g_1'' \ddot{g}_2 + \ddot{g}_1 g_2'' - 2\dot{g}_1' \dot{g}_2' \quad (A2)$$

For the initial nondimensional imperfection $\tilde{w} = -(\delta/t)\cos x$, the appropriate axisymmetric solution for the unbuckled cylinder is [4]

$$\begin{cases} w_0 = \left(\frac{v\lambda}{c}\right) - \left(\frac{\delta}{t}\right)\left(\frac{\lambda}{1-\lambda}\right)\cos x \\ f_0 = -\left(\frac{\lambda y^2}{2c}\right) + \left(\frac{\delta}{t}\right)\left(\frac{\lambda}{1-\lambda}\right)\cos x \end{cases} \quad (A3)$$

The postbuckling behavior will be represented by

$$\begin{cases} w = w_0 + \xi w_1 + \xi^2 w_2 + \dots \\ f = f_0 + \xi f_1 + \xi^2 f_2 \\ \lambda/\lambda_c = 1 + b\xi^2 + \dots \end{cases} \quad (A4)$$

where $|w_1|_{max} = 1$ and $\iint w_j w_1 \, dx \, dy = 0$ for $j \neq 1$. Substitution of (A4) into (A1) leads to the homogeneous equations

$$\begin{cases} \nabla^4 w_1 + 2\lambda_c w_1'' + f_1'' + \dfrac{\gamma \cos x}{1-\lambda_c}[\lambda_c \ddot{w}_1 - \ddot{f}_1] = 0 \\[4mm] \nabla^4 f_1 - w_1'' + \dfrac{\gamma \cos x}{1-\lambda_c}[\ddot{w}_1] = 0 \end{cases} \quad\quad \text{(A5)}$$

for the buckling eigenvalue λ_c and buckling mode (w_1, f_1); and to the equations

$$\begin{cases} \nabla^4 w_2 + 2\lambda_c w_2'' + f_2'' + \dfrac{\gamma \cos x}{1-\lambda_c}[\lambda_c \ddot{w}_2 - \ddot{f}_2] = 2c\psi(f_1, w_1) \\[4mm] \nabla^4 f_2 - w_2'' + \dfrac{\gamma \cos x}{1-\lambda_c}[\ddot{w}_2] = -c\psi(w_1, w_1) \end{cases} \quad\quad \text{(A6)}$$

for (w_2, f_2).

For the idealized case of an infinitely long cylinder, buckling solutions may be sought in the Floquet form[6]

$$\begin{cases} w_1 = \text{Ré}\,[w_{11}(x)\,e^{ikx/2}] \cos \dfrac{sy}{2} \\[4mm] f_1 = \text{Re}\,[f_{11}(x)\,e^{ikx/2}] \cos \dfrac{sy}{2} \end{cases} \quad\quad \text{(A7)}$$

where w_{11}, f_{11} are periodic in x, with period 2π, and, to satisfy circumferential periodicity, $(q_0 s/2)$ must be an integer. (This restriction on s will be dropped later.) The complex differential equations for w_{11} and f_{11} become

$$\begin{cases} \left(L_1^2 - \dfrac{s^2}{4}\right)^2 [w_{11}] + L_1^2[2\lambda_c w_{11} + f_{11}] - \dfrac{\gamma s^2 \cos x}{4(1-\lambda_c)}[\lambda_c w_{11} - f_{11}] = 0 \\[4mm] \left(L_1^2 - \dfrac{s^2}{4}\right)^2 [f_{11}] - L_1^2[w_{11}] - \dfrac{\gamma s^2 \cos x}{4(1-\lambda_c)}[w_{11}] = 0 \end{cases} \quad\quad \text{(A8)}$$

where

$$L_p[\ ] = [\ ]' + \frac{ipk}{2}[\ ] \quad\quad \text{(A9)}$$

It can be verified that all of the essentially different solutions correspond to values of k in the restricted range $[0, 1]$.

For given k and s, the solutions of (A6) have the forms

$$\begin{cases} w_2 = 2cs^2 \, \text{Re}\,\{w_{200}(x) + w_{220}(x)\,e^{ikx} + [w_{202}(x) + w_{222}(x)\,e^{ikx}]\cos sy\} \\[4mm] f_2 = 2cs^2 \, \text{Re}\,\{f_{200}(x) + f_{220}(x)\,e^{ikx} + [f_{202}(x) + f_{222}(x)\,e^{ikx}]\cos sy\} \end{cases} \quad\quad \text{(A10)}$$

Without loss of generality, it can be assumed that all of the functions $w_{11}, f_{11}, w_{200}, f_{200}$, etc. have Hermitian symmetry about $x = 0$ and $x = \pi$; thus

$$w_{11}(-x) = \overline{w_{11}(x)}$$
$$w_{11}(\pi + x) = \overline{w_{11}(\pi - x)}$$

and so on.

The four sets of differential equations governing the functions of x in (A10) are

$$\begin{cases} \left(L_p^2 - \dfrac{q^2 s^2}{4}\right)^2 [w_{2pq}] + L_p^2[2\lambda_c w_{2pq} + f_{2pq}] + \\[4mm] \quad - \dfrac{\gamma q^2 s^2 \cos x}{4(1-\lambda_c)}[\lambda_c w_{2pq} - f_{2pq}] = -(\tfrac{1}{16})R_{pq} \quad\quad \text{(A11a)} \\[6mm] \left(L_p^2 - \dfrac{q^2 s^2}{4}\right)^2 [f_{2pq}] - L_p^2[w_{2pq}] - \dfrac{\gamma q^2 s^2 \cos x}{4(1-\lambda_c)}[w_{2pq}] = (\tfrac{1}{32})S_{pq} \end{cases}$$

$$\text{(A11b)}$$
$$(p = 0,2; \quad q = 0,2)$$

where

$$\begin{aligned} R_{00} &= (w_{11}\bar{f}_{11})'' & S_{00} &= (w_{11}\bar{w}_{11})'' \\ R_{20} &= L_2^2[w_{11}f_{11}] & S_{20} &= L_2^2[w_{11}^2] \\ R_{02} &= L_2^2[w_{11}\bar{f}_{11}] - 4\bar{f}_{11}'L_2[w_{11}] & S_{02} &= L_2^2[w_{11}\bar{w}_{11}] - 4\bar{w}'L_2[w_{11}] \\ R_{22} &= w_{11}f_{11}'' + w_{11}''f_{11} - 2w_{11}'f_{11}' & S_{22} &= 2[w_{11}w_{11}'' - (w_{11}')^2] \end{aligned}$$

In solving the two sets of equations for $q = 0$, use must be made of the condition for single-valued circumferential displacement

$$\int_0^{2\pi R} \frac{\partial V}{\partial Y}\,dY = \int_0^{2\pi R}\left[\varepsilon_y - \frac{W}{R} - \frac{1}{2}\left(\frac{\partial W}{\partial Y}\right)^2\right]dY = 0$$

This gives

$$\int_0^{2\pi q_0}[f'' - vf - w - c\ddot{w}^2]\,dy = 0$$

which leads to the requirements

$$f_{200}'' = w_{200} + \tfrac{1}{32}(w_{11}\bar{w}_{11}) \quad\quad \text{(A12)}$$

and

$$L_2^2[f_{220}] = w_{220} + \tfrac{1}{32}(w_{11}^2) \quad\quad \text{(A13)}$$

These relations are consistent with equations (A11b) for $q = 0$, and their use in the corresponding equations (A11a) permits the determination of each of w_{200} and w_{220} from the uncoupled fourth order differential equations

$$w_{200}^{IV} + 2\lambda_c w_{200}'' + w_{200} = -\tfrac{1}{16}(w_{11}\bar{f}_{11})'' - \tfrac{1}{32}(w_{11}\bar{w}_{11}) \quad\quad \text{(A14)}$$

and

$$L_2^4[w_{220}] + 2\lambda_c L_2^2[w_{220}] + w_{220} = -\tfrac{1}{16}L_2^2[w_{11}f_{11}] - \tfrac{1}{32}(w_{11})^2 \quad (A15)$$

The pairs of functions (w_{202}, f_{202}) and (w_{222}, f_{222}) are governed by sets of two coupled fourth order equations.

The general formula displayed by Fitch[7] for the postbuckling coefficient b in problems involving nonlinear prebuckling states leads to the result, in the present problem,

$$\frac{b}{1-v^2} = \frac{6}{c\lambda_c} \frac{\langle Q[f_2, w_1, w_1] + 2Q[f_1, w_1, w_2]\rangle}{\langle 2(w_1')^2 + \dfrac{\gamma}{(1-\lambda_c)^2}[\dot{w}_1^2 \cos x - 2(\dot{f}_1 w_1' - f_1'^{\cdot}\dot{w}_1)\sin x]\rangle} \quad (A16)$$

where $Q[g_1, g_2, g_3] \equiv \ddot{g}_1 g_2' g_3' + g_1'' \dot{g}_2 \dot{g}_3 - g_1'^{\cdot}(\dot{g}_2 g_3' + g_2' \dot{g}_3)$, and $\langle \ \rangle$ represents averaging over the shell.

Note that for $k = l/m$, where l and m are integers, averages in the x direction may be computed via integrals with respect to x in the interval $[0, \pi m]$. But this process becomes inefficient for large m; fairly lengthy calculations show that except for $k = 0, \tfrac{1}{2}$ and 1, (A16) can be reduced to

$$\frac{b}{1-v^2} = \frac{3s^4}{8\lambda_c} \operatorname{Re} \int_0^\pi \Big\{ -8f_{202}|L_1(w_{11})|^2 - 4\bar{f}_{222}[L_1(w_{11})]^2 + \tfrac{3}{16}|w_{11}|^4 +$$

$$+2|w_{11}|^2(2w_{200} - f_{202}'') + w_{11}^2[2\bar{w}_{220} - \bar{L}_2^2(\bar{f}_{222})] +$$

$$-4f_{202}'[w_{11}\bar{L}_1(\bar{w}_{11}) + \bar{w}_{11}L_1(w_{11})] - 4w_{11}L_1(w_{11})\bar{L}_2(\bar{f}_{222}) +$$

$$-2[2w_{200}' + w_{202}'][f_{11}\bar{L}_1(\bar{w}_{11}) + \bar{f}_{11}L_1(w_{11})] +$$

$$-2f_{11}L_1(w_{11})\bar{L}_2[2\bar{w}_{220} + \bar{w}_{222}] + 4w_{202}[\bar{w}_{11}\bar{L}_1^2(f_{11}) +$$

$$+w_{11}\bar{L}_1^2(\bar{f}_{11})] + 4\bar{w}_{222}w_{11}L_1^2(f_{11}) - 2[2w_{200}' - w_{202}'] \times$$

$$\times [\bar{w}_{11}L_1(f_{11}) + w_{11}\bar{L}_1(\bar{f}_{11})] - 2w_{11}L_1(f_{11})\bar{L}_2(2\bar{w}_{220} - \bar{w}_{222}) +$$

$$-4w_{202}[\bar{L}_1(f_{11})L_1(\bar{w}_{11}) + \bar{L}_1(\bar{f}_{11})L_1(w_{11})] +$$

$$-4\bar{w}_{222}L_1(f_{11})L_1(w_{11})\Big\} dx$$

$$\div \int_0^\pi \Big\{ |L_1(w_{11})|^2 + \frac{\gamma s^2 \cos x}{8(1-\lambda_c)^2}[|w_{11}|^2 - 2\operatorname{Re}(w_{11}\bar{f}_{11})]\Big\} dx \quad (A17)$$

The cases $k = 0, \tfrac{1}{2}$ and 1 are exceptional because only for these values of k in the range [0,1] will one or both of the quantities e^{ikx} and e^{2ikx}, which appear in the evaluation of the Q functionals, have the same period 2π enjoyed by the solutions of (A11), (A14) and (A15). For $k = 1$ and $k = \tfrac{1}{2}$, (A16) may be used directly for the evaluation of b; the case $k = 0$, however, requires careful asymptotic treatment, and is analyzed in a later section of this Appendix.

The average shortening-per-unit-length Δ is

$$\Delta = -\left\langle \frac{\partial U}{\partial X}\right\rangle =$$

$$= \left\langle -\varepsilon_x + \frac{\partial W}{\partial X}\frac{\partial \tilde{W}}{\partial X} + \left(\frac{\partial W}{\partial X}\right)^2\right\rangle =$$

$$= \frac{t}{R}\left\langle -\bar{f} + 2c[w'\tilde{w}' + \tfrac{1}{2}(w')^2]\right\rangle$$

This gives the prebuckling axial stiffness at $\lambda = \lambda_c$ as

$$S_0 = \frac{1}{E}\left(\frac{d\sigma_0}{d\Delta_0}\right)_{\lambda=\lambda_c} = \left[1 + \frac{\gamma^2}{4(1-\lambda_c)^3}\right]^{-1} \quad (A18)$$

The initial postbuckling stiffness becomes

$$S = \frac{1}{E}\left(\frac{d\sigma}{d\Delta}\right)_{\lambda=\lambda_c} = \left[\frac{1}{S_0} + \frac{3}{4\pi\lambda_c}\left(\frac{1-v^2}{b}\right)I\right]^{-1}$$

where

$$I = \int_0^\pi |L_1(w_{11})|^2 \, dx \qquad \text{for } k \neq 1$$

$$= \int_0^\pi \left\{ |L_1(w_{11})|^2 + \frac{8\gamma s^2}{1-\lambda_c}\operatorname{Re}[L_2(w_{220})e^{ix} + w_{200}']\sin x\right\} dx \text{ for } k = 1$$

The postbuckling parameter α, given by equation (11) in terms of S and S_0, becomes

$$\alpha = \frac{2}{\pi}\arctan\left[\frac{4\pi\lambda_c}{3IS_0}\left(\frac{b}{1-v^2}\right)\right] \quad (A19)$$

For a given γ and k, the appropriate choice of s is that which minimizes λ_c; the restriction that $(q_0 s/2)$ be an integer was ignored in this minimization.

To find limiting results for $\gamma \to \infty$ we may set $s = 0$ in equations (A8) and (A11) but keep $\rho = \gamma s^2$ finite, and minimize λ_c with respect to ρ. It is evident, then, that $b/s^4(1-v^2)$ remains finite for $s \to 0$, so that the limiting value of α for $\gamma \to \infty$ is

$$(\alpha)_{\gamma=\infty} = \frac{2}{\pi}\arctan\left\{\frac{\pi\lambda_c\rho^2}{3I(1-\lambda_c)^3}\left[\frac{b}{s^4(1-v^2)}\right]\right\} \quad (A20)$$

Numerical analysis

Introduce the vector

$$Z = \begin{bmatrix} L_1^2(w_{11}) \\ w_{11} \\ L_1^2(f_{11}) \\ f_{11} \end{bmatrix} \quad (A21)$$

so that the buckling differential equations (A8), (A9) may be approximated in the range $[0, \pi]$ by the $(N+1)$ finite difference matrix equations

$$\bar{A}_1 Z_{n-1} + B_{11n} Z_n + A_1 Z_{n+1} = 0 \qquad (n = 0, 1, 2, \ldots, N) \tag{A22}$$

where A_p, a scalar, is

$$A_p = h^{-2} + \frac{ipk}{2} h^{-1} \tag{A23}$$

$$B_{pqn} = \begin{bmatrix} 2\lambda_c - \left(\dfrac{2}{h^2} + \dfrac{p^2 k^2}{4} + \dfrac{q^2 s^2}{2}\right) & \dfrac{q^4 s^4}{16} - \dfrac{\lambda_c \gamma q^2 s^2 \cos x_n}{4(1-\lambda_c)} & 1 & \dfrac{\gamma q^2 s^2 \cos x_n}{4(1-\lambda_c)} \\[2ex] -1 & -\left(\dfrac{2}{h^2} + \dfrac{p^2 k^2}{4}\right) & 0 & 0 \\[2ex] -1 & -\dfrac{\gamma q^2 s^2 \cos x_n}{4(1-\lambda_c)} & -\left(\dfrac{2}{h^2} + \dfrac{p^2 k^2}{4} + \dfrac{q^2 s^2}{2}\right) & \dfrac{q^4 s^4}{16} \\[2ex] 0 & 0 & -1 & -\left(\dfrac{2}{h^2} + \dfrac{p^2 k^2}{4}\right) \end{bmatrix} \tag{A24,}$$

and $h = \pi/N$.

The boundary conditions that reflect Hermitian symmetry about $x = 0$ and $x = \pi$ are

$$\begin{cases} Z_1 = Z_{-1} \\ Z_{N+1} = Z_{N-1} \end{cases} \tag{A25a} \tag{A25b}$$

A modified Potters' scheme[8] for solving (A22)* works as follows: let

$$Z_n = -P_n Z_{n+1} - Q_n Z_{n+1} \tag{A26}$$

Then, from (A22) it can be deduced that Q_n and P_n are given recursively by

$$\begin{cases} P_n = -A_1[\bar{A}_1 P_{n-1} - B_{11n} - A_1 \bar{A}_1 Q_{n-1}(A_1 \bar{P}_{n-1} - B_{11n})\bar{Q}_{n-1}]^{-1} \\ Q_n = -\bar{A}_1^2 A_1^{-1} P_n Q_{n-1}[A_1 \bar{P}_{n-1} - B_{11n}]^{-1} \end{cases} \tag{A27}$$

From (A25a) the initial conditions for (A27) are

$$\begin{cases} P_0 = A_1 B_{110}^{-1} \\ Q_0 = A_1 B_{110}^{-1} \end{cases} \tag{A28}$$

* The numerical solution was actually done for a vector Z whose components were defined in a slightly different way, but the set-up shown here is cleaner.

and, with the use of (A25b) it is found that Z_N must satisfy

$$E_N Z_N = 0 \tag{A29}$$

where

$$E_N = B_{11N} - \bar{A}_1(P_{N-1} + Q_{N-1}) - A_1(\bar{P}_{N-1} + \bar{Q}_{N-1}) \tag{A30}$$

The eigenvalues λ_c must, therefore, satisfy $|E_N| = 0$; the Z_n (to within a scalar factor) are then found from (A29) and subsequent back-substitution into (A26). Normalization is then imposed on Z to make $|w_1|_{max} = 1$; in all cases studied, this was the same as making $w_{11}(0) = 1$.

With

$$\zeta_p = \begin{bmatrix} L_p^2(w_{2p2}) \\ w_{2p2} \\ L_p^2(f_{2p2}) \\ f_{2p2} \end{bmatrix} \qquad (p = 0, 2) \tag{A31}$$

the difference equations governing ζ_p are (see eqs. (A11))

$$\bar{A}_p \zeta_{p,n-1} + B_{p2n}\zeta_{p,n} + A_p\zeta_{p,n+1} = -\tfrac{1}{16} T_{p,n} \tag{A32}$$

Here

$$T_{p,n} = \begin{bmatrix} R_{p2,n} \\ 0 \\ -\tfrac{1}{4}S_{p2,n} \\ 0 \end{bmatrix} \tag{A33}$$

and its elements are found with the use of numerical differentiation at x_n of the results found for w_{11} and f_{11}.

In the modified Potters' scheme for the nonhomogeneous equations (A32) and (A34)

$$\zeta_{p,n} = -P_n\zeta_{p,n+1} - Q_n\zeta_{p,n+1} + H_n \tag{A34}$$

and the recursive equations are the same as (A27) for P_n and Q_n, except that B_{11n} is replaced by B_{p2n} and A_p replaces A_1. The equation for H_n is

$$\begin{aligned} H_n = A_p^{-1}P_n[T_{p,n} - \bar{A}_pH_{n-1} + \\ -\bar{A}_pQ_{n-1}(A\bar{P}_{n-1} - B_{p2n})^{-1}(T_{p,n} - A_p\bar{H}_{n-1})] \end{aligned} \tag{A35}$$

The initial conditions are

$$\begin{cases} P_0 = A_p B_{p20}^{-1} \\ Q_0 = A_p B_{p20}^{-1} \\ R_0 = B_{p20}^{-1} T_{p,0} \end{cases} \tag{A36}$$

and the boundary conditions at $n = N$ give

$$\begin{aligned} \zeta_{p,N} = [B_{p2N} - \bar{A}_p(P_{N-1} + Q_{N-1}) + \\ -A_p(\bar{P}_{N-1} + \bar{Q}_{N-1})]^{-1}[T_{p,N} - \bar{A}_pH_{N-1} - A_p\bar{H}_{N-1}] \end{aligned} \tag{A37}$$

Back substitution into (A34) provides the rest of the $\zeta_{p,n}$.

The numerical solution for w_{200} and w_{220} proceeds in a simpler, but analogous, fashion on the basis of the fourth order differential equations (A14) and (A15).

The evaluation of $b/(1-v^2)$ and α was executed by means of straight-forward numerical integration. It may be mentioned that for a few fractional values of $k=1/m$ other than $\frac{1}{2}$, $b/(1-v^2)$ was evaluated both by equation (A17) and by the direct use of (A16) with the longitudinal averages taken over the interval $[0, m\pi]$; the agreement was good.

The results for $\gamma \to \infty$ were found simply by replacing the combination of terms (γs^2) in B_{pqn} by ρ, but setting $s=0$ elsewhere in B_{pqn}. Then λ_c was minimized with respect to ρ and the rest of the calculations proceeded routinely, with equation (A20) used to find $(\alpha)_{\gamma=\infty}$. It should be mentioned that all of the solutions to the difference equations varied quite smoothly in $[0, \pi]$ so that calculation with $N=30$ provided adequate accuracy. Finally, it can be seen that for $k=1$, the eigenvalue λ_c is degenerate, since, if w_{11} is an eigenfunction, so is $\bar{w}_{11} e^{-ix}$; the computational difficulties associated with this degeneracy were avoided by reformulating the eigenvalue problem in terms of $(w_{11} e^{ikx/2})$.

Asymptotic analysis for $k \to 0$

In the case of the perfect cylinder, equation (4) shows that the circumferential wave number s_0 approaches $\sqrt{2k}$ as k vanishes; a similar quadratic relation between s and k is anticipated for the imperfect cylinder. Hence, in the differential equations (A8) and (A11) let $k=\tau s^2/2$; this requires the replacement of the operator L_p by $\mathcal{L}_p$, where

$$\mathcal{L}_p[\ ] = [\ ]' + \frac{ip\tau s^2}{4}[\ ]$$ (A38)

Expand the various displacements and stress-functions into the forms

$$w_{11} = w_{11}^{(0)} + s^2 w_{11}^{(1)} + s^4 w_{11}^{(2)} + \cdots$$
$$f_{11} = f_{11}^{(0)} + s^2 f_{11}^{(1)} + s^4 f_{11}^{(2)} + \cdots$$ (A39)

and

$$w_{2pq} = w_{2pq}^{(0)} + s^2 w_{2pq}^{(1)} + s^4 w_{2pq}^{(2)} + \cdots$$
$$f_{2pq} = f_{2pq}^{(0)} + s^2 f_{2pq}^{(1)} + s^4 f_{2pq}^{(2)} + \cdots \quad (p=0,2: q=0,2)$$ (A40)

where $w_{11}(0)=1$, and $\langle w_{11} w_{11} \rangle = 0$ for $j \neq 1$. Further, write λ_c as

$$\lambda_c = \lambda_0 + s^2 \lambda_1 + \cdots$$ (A41)

Substitution of (A39) and (A41) into the modified buckling equations (A8) and execution of a perturbation calculation that repeatedly invokes peri-

odicity of the solution leads to the following results:

$$w_{11}^{(0)} = a_1 \qquad w_{11}^{(1)} = b_1 \cos x$$
$$f_{11}^{(0)} = c_1 \qquad f_{11}^{(1)} = d_1 \cos x + \text{(constant)}$$ (A42)

where a_1, b_1, c_1, d_1 satisfy

$$M_{11} \begin{bmatrix} a_1 \\ c_1 \\ b_1 \\ d_1 \end{bmatrix} = 0$$ (A43)

with

$$M_{pq} = \begin{bmatrix} q^4 - 2\lambda_0 p^2 \tau^2 & -p^2\tau^2 & -\dfrac{2\lambda_0\gamma q^2}{1-\lambda_0} & \dfrac{2\gamma q^2}{1-\lambda_0} \\[2ex] -p^2\tau^2 & -q^4 & \dfrac{2\gamma q^2}{1-\lambda_0} & 0 \\[2ex] -\dfrac{2\lambda_0\gamma q^2}{1-\lambda_0} & \dfrac{2\gamma q^2}{1-\lambda_0} & 8(1-2\lambda_0) & -8 \\[2ex] \dfrac{2\gamma q^2}{1-\lambda_0} & 0 & -8 & -8 \end{bmatrix}$$ (A44)

The vanishing of the determinant $|M_{11}|$ then gives the characteristic equation for λ_0 as

$$8(1-\lambda_0)^5(1-2\lambda_0\tau^2+\tau^4)+2\gamma^2(1-\lambda_0)^2[2(1-\tau^2)+$$
$$-4\lambda_0(1+\tau^2)-\lambda_0^2]+\gamma^4=0$$ (A45)

Minimization of λ_0 with respect to τ gives

$$\tau^2 = \lambda_0 + \frac{\gamma^2(1+2\lambda_0)}{4(1-\lambda_0)^3}$$ (A46)

and then

$$\gamma^4(1-6\lambda_0-4\lambda_0^2)+4\gamma^2(1-\lambda_0)^3(2-6\lambda_0-5\lambda_0^2)+16(1-\lambda_0)^7(1+\lambda_0)=0$$ (A47)

This is an exact equation for λ_0, giving the result for $k \to 0$ plotted in figure 1. The perturbation procedure applied to the modified equations (A11) provides the following results for w_{2p2} and f_{2p2} ($p=0,2$):

$$w_{2p2}^{(0)} = a_p \qquad w_{2p2}^{(1)} = b_p \cos x + \text{(constant)}$$
$$f_{2p2}^{(0)} = c_p \qquad f_{2p2}^{(1)} = d_p \cos x + \text{(constant)}$$ (A48)

where

$$M_{p2}\begin{Bmatrix} a_p \\ c_p \\ b_p \\ d_p \end{Bmatrix} = \frac{1}{2}\begin{vmatrix} 2a_1c_1 \\ 4b_1d_1 \\ 2b_1^2 \\ c_1b_1+a_1d_1 \\ a_1b_1 \end{vmatrix} + \frac{(2-p)\tau^2}{16}\begin{vmatrix} a_1^2 \\ 0 \\ 0 \end{vmatrix} \quad (p=0,2) \quad (A49)$$

must be solved for (a_p, c_p, b_p, d_p). (The terms shown as (constant) in (A42) and (A48) will not be needed in the ultimate determination of the post-buckling parameter α.)

Finally, the results for w_{200} and w_{220} found by perturbation solution of equations (A14) and (A15) are

$$\overset{(0)}{w_{2p0}} = -\frac{a_1^2}{32}$$

$$\overset{(1)}{w_{2p0}} = -\left[\frac{a_1b_1-a_1d_1-c_1b_1}{32(1-\lambda_0)}\right]\cos x \quad (A50)$$

$$\overset{(2)}{w_{2p0}} = -\left[\frac{b_1^2}{64} + \frac{p^2\tau^2}{256}a_1(\lambda_0 a_1 - c_1)\right] + (T_p) \quad (p=0,2)$$

The terms (T_p) are trigonometric functions that will not affect α.

In evaluation of the right hand side of (A49) and (A50), the constants (a_1, b_1, c_1, d_1) are the solution of (A43) corresponding to the values of λ_0 and τ that satisfy (A47) and (A46). The normalization $\overset{(0)}{w_{11}}(0) = 1$ implies that $a_1 = 1$; this value for a_1 and the associated results for b_1, c_1, d_1 were used consistently.

Evaluation of $b/(1-\nu^2)$ by equation (A17) reveals that $b = 0(s^4)$ for $s \to 0$, with the result

$$\left[\frac{b}{s^4(1-\nu^2)}\right] \approx -\frac{6}{\lambda_0}\left\{-\frac{3}{16}(1-\lambda_0)^{-1}(a_1b_1-a_1d_1-c_1b_1)^2 + \right.$$
$$+ \frac{\tau^2 a_1}{32}(-16a_1c_0 - \lambda_0 a_1^3 + 2a_1^2c_1 - 32c_1a_0) + \frac{3}{8}a_1^2b_1^2 +$$
$$- (c_1b_1+a_1d_1)(2b_0+b_2) - a_1b_1(2d_0+d_2) - 2b_1^2(2c_0+c_2) +$$
$$\left. -4b_1d_1(2a_0+a_2)\right\} \div \left\{8b_1^2 + \tau^2a_1^2 + \frac{2\gamma}{1-\lambda_0}(a_1b_1-a_1d_1-c_1b_1)\right\}$$

$$(A51)$$

The formula for α becomes

$$\alpha = \frac{2}{\pi}\arctan\left\{\frac{64\lambda_0}{3S_0(8b_1^2+\tau^2a_1^2)}\left[\frac{b}{s^4(1-\nu^2)}\right]\right\} \quad (A52)$$

In the limit $\gamma \to \infty$, $\lambda_0 \to 0.1516$, and

$$\left(\frac{\tau}{\gamma}\right)^2 \to \frac{1+2\lambda_0}{4(1-\lambda_0)^3}.$$

It is found that a_p, c_p, (b_p/γ) and (d_p/γ) $(p=0,1,2)$ remain bounded and that $b/s^4(1-\nu^2)$ approaches a finite limit as $\gamma \to \infty$. The formula for α for $\gamma = \infty$ becomes

$$\alpha = \frac{2}{\pi}\arctan\left\{\frac{16\lambda_0}{3(1-\lambda_0)^3\left[8\left(\frac{b_1}{\gamma}\right)^2 + \left(\frac{\tau}{\gamma}\right)^2\right]a_1^2}\left[\frac{b}{s^4(1-\nu^2)}\right]\right\} \quad (A53)$$

REFERENCES

1. NASA, *Buckling of Thin-Walled Circular Cylinders*, NASA SP-8007, August 1968.
2. Weingarten, V.I., Morgan, E.J., and Seide, P., 'Elastic Stability of Thin-Walled Cylindrical and Conical Shells under Axial Compression', *AIAA Journal*, Vol. 3, 1965, pp. 500–506.
3. Hoff, N.J., Madsen, W.A., and Mayers, J., 'Post-buckling Equilibrium of Axially Compressed Circular Cylindrical Shells', *AIAA Journal*, Vol. 4, 1966, pp. 126–133.
4. Koiter, W.T., 'The Effect of Axisymmetric Imperfections on the Buckling of Cylindrical Shells under Axial Compression', *Proceedings, Koninkl. Nederl. Akademie van Wetenschappen*, Vol. 66, Series B, No. 5, 1963, pp. 265–279.
5. Almroth, B.O., *Influence of Imperfections and Edge Restraint on the Buckling of Axially Compressed Cylinders*, NASA CR–432, April 1966.
6. Stoker, J.J., *Nonlinear Vibrations*, Interscience, N.Y., 1950, p. 193.
7. Fitch, J.R., 'The Buckling and Postbuckling Behavior of Spherical Caps under Concentrated Load', *Int. Journal Solids and Structures*, Vol. 4, 1968, pp. 421–446.
8. Potters, M.L., *A Matrix Method for the Solution of a Second Order Difference Equation in Two Variables*, Report MR 19, Mathematisch Centrum, Amsterdam, 1955.